Thymidine Metabolism as Confounding Factor of 3'-Deoxy-3'-[^{18}F]Fluorothymidine Uptake after Therapy in a Colorectal Cancer Model

Sonja Schelhaas[1], Lydia Wachsmuth[2], Sven Hermann[1], Natascha Rieder[3], Astrid Heller[3], Kathrin Heinzmann[4], Davina J. Honess[5], Donna-Michelle Smith[5], Inga B. Fricke[1], Nathalie Just[2], Sabrina Doblas[6], Ralph Sinkus[7], Christian Döring[1], Klaus P. Schäfers[1], John R. Griffiths[5], Cornelius Faber[2], Richard Schneider[8], Eric O. Aboagye[4,*] and Andreas H. Jacobs[1,9,*]

[1] European Institute for Molecular Imaging (EIMI), Westfälische Wilhelms-Universität Münster, Münster, Germany

[2] Department of Clinical Radiology, University Hospital of Münster, Münster, Germany

[3] Roche Pharma Research and Early Development, Pathology and Tissue Analytics, Roche Innovation Center Munich, Germany

[4] Comprehensive Cancer Imaging Centre, Imperial College London, UK

[5] Cancer Research UK Cambridge Institute, Cambridge, UK

[6] Laboratory of imaging biomarkers, UMR 1149 - CRI, Inserm, Paris Diderot University, Paris, France

[7] Imaging Sciences & Biomedical Engineering Division Kings College, London, UK

[8] Merck KGaA, Darmstadt, Germany

[9] Department of Geriatric Medicine, Johanniter Hospital, Bonn, Germany

[*]equal contribution

Corresponding Authors:

Andreas H. Jacobs, European Institute for Molecular Imaging, Waldeyerstr. 15, 48149 Münster, Germany, Phone: +492518349300, Fax: +492518349313, Email: ahjacobs@uni-muenster.de

Eric O. Aboagye, Comprehensive Cancer Imaging Centre, Department of Surgery and Cancer, Faculty of Medicine, Imperial College London, Hammersmith Hospital, Du Cane Road, London, W12 0NN, UK, Phone: +442033133759; Fax: +442083831783; Email: eric.aboagye@imperial.ac.uk

First Author:

Dr. Sonja Schelhaas (Postdoc), European Institute for Molecular Imaging, Waldeyerstr. 15, 48149 Münster, Germany, Phone: +492518349312, Fax: +492518349313, Email: sonja.schelhaas@uni-muenster.de

Financial support: The research leading to these results has received support from the Innovative Medicines Initiative Joint Undertaking (www.imi.europa.eu) under grant agreement number 115151, resources of which are composed of financial contribution from the European Union's Seventh Framework Programme (FP7/2007-2013) and EFPIA companies' in kind contribution. This work was also supported by the Deutsche Forschungsgemeinschaft (DFG), Cells-in-Motion Cluster of Excellence (EXC1003 – CiM), University of Münster, the Interdisciplinary Centre for Clinical Research (IZKF, core unit PIX), Münster, Germany and core funding from Cancer Research UK – C2536/A16584.

Word count: 4999

Running title: FOLFOX combination therapy in CRC models

ABSTRACT

Non-invasive monitoring of tumor therapy response helps in developing personalized treatment strategies. Here, we performed sequential positron emission tomography (PET) and diffusion-weighted magnetic resonance imaging (DW-MRI) to evaluate changes induced by a FOLFOX-like combination chemotherapy in colorectal cancer (CRC) xenografts, to identify the cellular and molecular determinants of these imaging biomarkers.

Methods: Tumor bearing CD1 nude mice, engrafted with FOLFOX-sensitive Colo205 CRC xenografts, were treated with FOLFOX (5-fluorouracil, leucovorin and oxaliplatin) in weekly intervals. On d1, d2, d6, d9 and d13 of therapy, tumors were assessed by *in vivo* imaging and *ex vivo* analyses. In addition, HCT116 xenografts, which did not respond to the FOLFOX treatment, were imaged on d1 of therapy.

Results: In Colo205 xenografts, FOLFOX induced a profound increase in uptake of the proliferation PET tracer 3'-deoxy-3'-[^{18}F]fluorothymidine ([^{18}F]FLT), which was accompanied by increases in markers for proliferation (Ki67, TK1) and for activated DNA damage response (DDR; γH2AX), whereas the effect on cell death was minimal. As tracer uptake was unaltered in the HCT116 model, these changes appear to be specific for tumor response.

Conclusion: We demonstrate that [^{18}F]FLT PET can non-invasively monitor molecular alterations induced by a cancer treatment, including thymidine metabolism and DDR. The cellular or imaging changes may not, however, be directly related to therapy response as assessed by volumetric measurements.

Key words: [^{18}F]FLT PET, DW-MRI, combination cancer therapy, small animal imaging

Colorectal cancer (CRC) is the third most common cancer and the fourth most common cause for cancer related deaths worldwide (*1*). FOLFOX, the combination of oxaliplatin, 5-fluorouracil (5-FU) and leucovorin (folinic acid), is a frequently employed therapy for CRC. The active metabolites of 5-FU disrupt RNA synthesis and inhibit thymidylate synthase (TS), an enzyme important for DNA synthesis. This TS inhibitory activity can be enhanced by leucovorin (*2*). The combination of these two agents has been shown to be superior to therapy with 5-FU alone in patients with advanced CRC (*3*). Oxaliplatin is a third generation platinum analogue, inducing DNA intra- and inter-strand crosslinks, which ultimately results in cell death (*4*). The addition of oxaliplatin to the combination of 5-FU and leucovorin is beneficial for outcome for instance in the adjuvant (*5*) setting.

Molecular imaging can aid in early and non-invasive identification of patients not responding to therapy, allowing an early change of the treatment approach. This not only results in the reduction of unnecessary side effects for the patient, but also allows for early definition of effective treatment. Positron emission tomography (PET) with 2-[^{18}F]-fluoro-2-deoxy-D-glucose ([^{18}F]FDG) is routinely used in the clinic for tumor therapy follow-up. A drawback of [^{18}F]FDG is its accumulation in inflammatory lesions (*6*). The proliferation tracer 3'-deoxy-3'-[^{18}F]fluorothymidine ([^{18}F]FLT), a thymidine analogue, performs better than [^{18}F]FDG with regards to selectivity. It has already been successfully employed for monitoring tumor response to therapy in a range of preclinical and clinical studies (*7,8*). [^{18}F]FLT is phosphorylated by thymidine kinase 1 (TK1) and retained within proliferative cells. Therefore, its uptake reflects the thymidine salvage pathway (*9*), an alternative thymidine-to-DNA pathway to the *de novo* pathway, with the key enzyme TS. Thymidine phosphorylase (TP) affects [^{18}F]FLT uptake by degrading thymidine, whereas [^{18}F]FLT is resistant to the activity of this enzyme (*10*). It is well recognized that thymidine competes with [^{18}F]FLT for cellular retention (*11*) and that this competition can be modified by TP (*12,13*). Moreover, TP activity plays a role in tumor angiogenesis, induces metastasis, and protects cancer cells against apoptosis (*14*).

Another method for non-invasive monitoring of response to therapy is diffusion-weighted MRI (DW-MRI). Tumor cell killing as a consequence of successful therapy results in increased intercellular space and hence enhanced water diffusion, measured as an increase in the apparent diffusion coefficient (ADC) (*15*).

Here, we employed CRC models treated with a FOLFOX-like combination therapy, which we refer to as FOLFOX. We evaluate changes in uptake of the radiotracers [^{18}F]FLT and [^{18}F]FDG, as well as in ADC measured by DW-MRI, and analyze associated alterations within the tumors on a cellular level. This will allow a better understanding of tumor biology and factors affecting imaging biomarkers, paving the way for improved cancer therapy in the clinical setting.

MATERIALS AND METHODS

Animal model

Colo205 and HCT116 cells were cultivated in DMEM or RPMI, respectively, supplemented with 10 % fetal calf serum and 100 U/mL penicillin and 100 µg/mL streptomycin. Animal procedures were performed in accordance with the German Laws for Animal Protection and were approved by the animal care committee of the local government (North Rhine-Westphalia State Agency for Nature, Environment and Consumer Protection). 5 x 10^6 Colo205 or 2 x 10^6 HCT116 cells were injected subcutaneously into the shoulder region of 6 to 8 week old female CD1 nude mice (Charles River Laboratories). Two tumors were inoculated per animal and growth was followed by digital caliper measurements (volume = ½ (length * width^2)).

Animals were assigned randomly into groups. FOLFOX therapy was applied at weekly intervals. The treatment was started with oxaliplatin (8 mg/kg, intraperitoneal) followed by leucovorin 1.5 h later (90 mg/kg, retrobulbar) and two doses of 5-FU (30 mg/kg at 2 h and 6 h after treatment initiation, intraperitoneal). All agents were obtained from the pharmacy of the University Hospital of Münster. Control animals were injected with the respective solvents at the same time points. 5-FU therapy consisted of two doses of 5-FU only (30 mg/kg each, given 4 h apart). The experimental schedule is presented in **Supplemental Table 1**.

[^{18}F]FLT PET imaging and analysis

[^{18}F]FLT was synthesized as reported previously (*16*). 10 MBq of tracer was injected into isoflurane anaesthetized mice. Imaging was performed 70 min - 90 min after tracer application using a quadHIDAC PET (Oxford Positron Systems, UK). A multimodal bed was used that was transferred to a Bruker MR

tomograph during the tracer acquisition period (for DW-MR imaging, see below), or to a CT scanner (Inveon, Siemens Medical Solutions, USA) after completion of the PET scan.

Volumes of interest (VOIs) were drawn manually on anatomical images and transferred to the respective PET images using the in-house developed software for multimodal data analysis - MEDgical. The whole tumor was defined by the VOI and tracer uptake was expressed as SUV_{max}. Also other modes of quantification were performed, as shown in the **Supplemental Material**. These data confirm that the results and conclusions are not dependent on the method of analysis.

DW-MR imaging

A Bruker Biospec 9.4 T tomograph was employed to obtain data on water diffusion. First, T2-weighted images were acquired (2D rapid acquisition with relaxation enhancement (RARE), TR/TE 3600/40 ms, Rare factor 8, FOV 35 mm, 256 matrix, slice thickness 1 mm, 4 slices per tumor at biggest tumor diameter), followed by DW images (EPI-DTI, TR/TE 1000/19 ms, 12 segments, 7 b-values from 0 - 700 s/mm², 128 matrix, NEX 6, respiration-triggered). Analysis of ADC values was performed with the software Beaugui developed at INSERM. ADC maps were calculated on a pixel-by-pixel basis using ROOT-based data analysis software (ROOT, v5.34.01; CERN, Geneva, Switzerland). The ADC was calculated by fitting the normalized signal intensity to a classical monoexponential model (cut-off > 150 s/mm^2), using a non-linear least square approach with a Levenberg-Marquardt algorithm. Tumor ROIs were defined manually on the b = 0 images and then copied onto the ADC maps to determine ADC_{mean}.

Immunohistochemistry

Formalin-fixed tumor tissue was stained and analyzed as described in detail in the **Supplemental Methods**.

Thymidine analysis

Thymidine in tumors and plasma was quantified as described previously (*17*).

Statistics

Results are expressed as boxplots showing the median and the 25%ile and 75%ile. Error bars depict the maximum and minimum values. Mean and standard deviation were plotted for correlation analyses. Significances were calculated with the software SigmaPlot 13. Since not all data were normally distributed, we used the Mann-Whitney rank sum test to compare groups. Correlations were determined with the Spearman correlation coefficient. All numerical data and sample sizes are presented in the **Supplemental Material**.

RESULTS

Molecular imaging of treatment response in Colo205 xenografts

We established a FOLFOX treatment regime that closely resembles the therapy schedule employed in the clinical situation. When given at weekly intervals, the therapy resulted in growth inhibition of Colo205 xenografts (**Fig. 1A, Supplemental Table 2**), implying that these tumors are sensitive to FOLFOX.

[^{18}F]FLT PET imaging revealed a remarkable increase of tracer uptake in FOLFOX treated Colo205 xenografts at all time points investigated (**Figs. 1B and C, Supplemental Table 3**). The largest increase was observed one day after therapy (9.2-fold relative to baseline, 10.1-fold relative to control). At the end of a treatment cycle (d6 and d13) tracer uptake approached baseline levels, but was still significantly enhanced. A potential cause of increased [^{18}F]FLT could be the TS inhibitory activity of 5-FU. Therefore, we analyzed [^{18}F]FLT uptake in tumors treated with 5-FU on the first day of therapy, when the strongest induction of [^{18}F]FLT accumulation could be observed after combination therapy. 5-FU caused a remarkable increase in [^{18}F]FLT uptake (SUV_{max}: control: 1.6 ± 0.4, 5-FU: 11.6 ± 2.5, $P < 0.01$, 7.1-fold relative to control, **Fig. 1C**). However, the FOLFOX combination resulted in an even stronger increase (SUV_{max}: 16.5 ± 2.0, $P < 0.01$ relative to 5-FU), indicating that 5-FU alone is not responsible for the total extent of [^{18}F]FLT uptake after FOLFOX therapy.

We also performed longitudinal DW-MRI studies on FOLFOX treated tumors (**Fig. 1D, Supplemental Table 4**). The resulting ADC maps show a variable and heterogeneous distribution of water diffusion (**Supplemental Fig. 1**). Tumors tended to have lower ADC values over time, irrespective of treatment.

Relative to baseline, the ADC_{mean} of FOLFOX treated tumors was significantly decreased on d2, d6, d9 and d13 and the ADC_{mean} of control treated tumors was significantly decreased on d9. Tumors of FOLFOX treated mice tended to have higher ADC values compared to tumors of control treated animals, an effect that was significant on d9. 5-FU treatment alone did not result in changes of water diffusion on day one.

Ex vivo analyses of FOLFOX treated Colo205 xenografts

Immunohistochemistry showed an increase of Ki67 and TK1 staining in the FOLFOX treated tumors (**Fig. 2, Supplemental Table 5**), implying an increase of cellular proliferation. Elevated TK1 staining was also noted on day 1 when mice were treated with 5-FU alone. No statistically significant association of [^{18}F]FLT with Ki67 immunohistochemistry could be detected. However, a correlation with TK1 (ρ = 0.893, P < 0.001) was observed.

Western blot analysis confirmed an increase in TK1 expression after FOLFOX therapy and also indicated upregulation of the other thymidine metabolism proteins TS and TP (**Supplemental Fig. 2** and **Supplemental Table 6**). This prompted us to analyze the levels of thymidine within tumors and in the plasma, which were both decreased at later time points in FOLFOX treated animals (**Fig. 3** and **Supplemental Table 7**).

Immunohistochemical analysis of cleaved caspase-3 and a TUNEL assay revealed an increased level of cell death only after the second treatment (d9 and d13, **Fig. 4, Supplemental Table 8**). Other histological markers of cell death were not altered (**Supplemental Fig. 3**).

Many therapeutic agents induce double-strand breaks in DNA, which result in activation of cellular DNA damage response (DDR) mechanisms. A key step of DDR is phosphorylation of the histone variant H2AX, producing γH2AX, which is required for assembly of DNA repair proteins (*18*). Analysis of γH2AX revealed prolonged activation of DDR post FOLFOX treatment in Colo205 xenografts, and also one day after 5-FU treatment (**Fig. 5, Supplemental Table 9**). [^{18}F]FLT uptake was correlated with γH2AX staining (ρ = 0.964, P < 0.001).

[^{18}F]FLT PET imaging of non-responsive HCT116

HCT116 xenografts appear to be non-responsive to FOLFOX, as their growth was not impaired even after three cycles of therapy (**Fig. 6A, Supplemental Table 10**). We analyzed changes of [^{18}F]FLT on day one after therapy, as [^{18}F]FLT increase was most pronounced at this time point. No alteration of [^{18}F]FLT was observed in HCT116 tumors (**Fig. 6B, Supplemental Table 11**).

DISCUSSION

Longitudinal molecular imaging in conjunction with *ex vivo* molecular analyses were performed to investigate alterations induced by a FOLFOX-like combination therapy in CRC models in a clinically translatable approach. FOLFOX induced a substantial increase in [^{18}F]FLT uptake, corresponding to sustained increases in DDR and proliferation markers. In contrast, [^{18}F]FLT was unaltered in non-responding HCT116 xenografts implying that the observed increase is predictive for therapy response. Prolonged activation of DDR is most likely responsible for the absence of any major changes in tumor cell death, which are reflected by unaltered water diffusivity, as assessed by DW-MRI. We speculate that the observed alterations are based on this tumor possessing a DNA repair-proficient metabolic phenotype, with delayed onset of cell death involving enhanced requirements for nucleosides via the salvage pathway.
Since [^{18}F]FLT PET is thought to report tumor proliferation and DW-MRI is sensitive to the increase in ADC as a consequent of cell death, the two methods are complementary, particularly for monitoring the response of tumors to chemotherapy. This allows a comprehensive assessment of the biological processes engaged, potentially improving care of cancer patients, especially when the two imaging modalities are conducted in combination.

Increase in [^{18}F]FLT uptake in FOLFOX treated xenografts was remarkable. As growth was arrested in the treated tumors, one would expect a decrease in uptake of this proliferation tracer rather than an increase. In addition, we observed a significant increase in Ki67 immunohistochemical staining. This increased Ki67 staining is in contradiction to the normal expectation of reduced proliferation in tumors that arrest in growth. However, it is in line with a clinical study that observed increased Ki67 expression in CRC liver metastases after FOLFOX therapy. The authors concluded that this increase could have resulted from increased

proliferation and migration induced by an autocrine mechanism which might be used by metastatic cells escaping FOLFOX-induced cell death (*19*). Possibly in our tumor model the Ki67 signal arose from proliferative tumor cells that increased in number relative to non-proliferating tumor cells. Tumor volume measurements show that even though in the third treatment week tumor volumes were still significantly reduced relative to controls, the tumors tended to grow again. This could possibly imply that there are indeed proliferative tumor cells present in the FOLFOX-treated xenografts.

Western blot analysis implied that TP, TS and TK1 were also upregulated, even though they are involved in opposing thymidine pathways. These results were not statistically significant using non-parametric tests, likely due to the low sample number. However, it is likely that they are of biological relevance. TS might be upregulated as a mechanism of resistance to 5-FU therapy (*20*), and oxaliplatin has been shown to increase expression of TP (*21*). Increased TK1 expression was in line with respective TK1 immunohistochemistry. It has already been reported that inhibition of TS by 5-FU can induce upregulation of TK1, resulting in increased accumulation of [^{18}F]FLT (*22*). In our study, TK1 expression parallels [^{18}F]FLT uptake. At the end of a treatment cycle, both approached the levels of controls, implying that tumor biology recedes back to baseline levels. This could be caused by the limited plasma half-lives of the therapeutic agents used.

Thymidine within tumors and plasma was decreased on d6, d9 and d13, which could be provoked by the catalytic activity of TP (*10*). Furthermore, TS-inhibitory agents like 5-FU can induce the thymidine salvage pathway, resulting in enhanced utilization of thymidine (*23*). In our model, diminished levels of thymidine might also contribute to the increased uptake of [^{18}F]FLT in tumors, as thymidine and [^{18}F]FLT compete for cellular uptake and retention (*11*).

Most of the observed changes (upregulation of thymidine pathway enzymes and [^{18}F]FLT) can probably be attributed to the action of 5-FU. However, we demonstrated that equivalent doses of 5-FU alone lead to a less pronounced increase in [^{18}F]FLT than the increase provoked by FOLFOX, suggesting that in our therapy model TS inhibition is amplified relative to that caused by 5-FU alone. Leucovorin stabilizes the complex of 5-FU with TS. Furthermore, it is likely that oxaliplatin-induced increase of TP expression results in improved activity of 5-FU, as TP converts 5-FU to one of its active metabolites, 5-fluoro-2'-deoxyuridine

(*14*). It will be interesting to investigate in future experiments, whether the differences in TS inhibition and [^{18}F]FLT uptake are related to differences in tumor growth inhibition.

The increase in [^{18}F]FLT uptake in the FOLFOX-responsive Colo205 model appears to be predictive for therapy response, as [^{18}F]FLT was unchanged in the non-responsive HCT116 xenografts. Consequently, an increase in [^{18}F]FLT accumulation is possibly a prognostic marker for this treatment approach. This hypothesis is strengthened by a clinical feasibility study by Kenny et al., measuring [^{18}F]FLT uptake one hour after treatment with the 5-FU prodrug capecitabine, showing that tracer uptake parameters did not change in breast cancer patients who progressed on therapy, whereas they were increased in responders (*24*). In contrast, Hong et al. observed an increase in [^{18}F]FLT uptake on d2 after FOLFOX treatment initiation in CRC patients, which was more pronounced in non-responders than in responders (*25*). Some clinical and preclinical studies have shown that non-therapeutic doses of TS-inhibitory agents can also cause an increase in [^{18}F]FLT (*26–28*), indicating that this change is not predictive of tumor response to TS-inhibiting agents. Thus, further investigations are needed, to assess the role of [^{18}F]FLT in the prediction of tumor therapy response when employing agents inhibiting TS.

In Colo205 xenografts, we also performed PET imaging with the clinically established metabolism tracer [^{18}F]FDG (**Supplemental Fig. 4, Supplemental Table 12**). [^{18}F]FDG uptake was not consistently altered, therewith not reflecting FOLFOX effects. Moreover, [^{18}F]FDG accumulates in inflammatory lesions, so the unchanged [^{18}F]FDG also implies that the increase in [^{18}F]FLT observed in this study was not caused by inflammatory cells.

In our study, tumor cell death was only slightly increased within the second FOLFOX treatment cycle, as measured by caspase-3 IHC and TUNEL. In contrast, other histological markers of cell death (cellular density, necrotic area) were unaltered. These results provide a plausible explanation for why we did not detect a FOLFOX-induced increase of ADC_{mean}. The observed differences in water diffusion occurred at all time points investigated, and do not appear to be of physiological relevance.

Histological analysis revealed sustained activation of the DDR marker H2AX after FOLFOX or 5-FU therapy, which could be caused by oxaliplatin or 5-FU (*29,30*). 5-FU induced DDR has been described to occur in S-phase (*31*). Hence, it is likely that also the DDR observed here is linked to this phase, which is in line with sustained TK1 expression, which is S-phase specific. In our study, elevated γH2AX was observed at all time points, even though levels approached those of control levels at the end of the first treatment cycle (d6). Decreasing γH2AX expression might suggest either successful repair of the DNA damage, or lysis of dead cells (*32*). As no induction of cell death was observed on d6 after FOLFOX and immunohistochemical markers of proliferation were increased, it is likely that the DNA damage was successfully repaired. Hence, attempts of the tumor cell to repair DNA double-strand breaks might delay induction of cell death, explaining unchanged ADC_{mean}.

Increased amounts of nucleosides are needed during DDR. Consequently, DDR in the treated tumors could potentially contribute to the increased [^{18}F]FLT uptake observed here. γH2AX expression parallels [^{18}F]FLT uptake and we detected a correlation of [^{18}F]FLT uptake and γH2AX expression, supporting our hypothesis of increased nucleoside consumption during DDR.

A limitation of this study is that we did not evaluate tumors treated with single agents, apart from the analysis of a single time point for 5-FU. Such an analysis would help to assess the relative contribution of each agent to the observed changes. However, single agents are rarely employed in the clinical setting. Therefore, our data shed light on changes induced by a clinically relevant therapy approach. It would be of interest to assess FOLFOX induced mechanisms in a broader panel of tumor types including non-responsive models and clinical tumor specimens.

CONCLUSION

Factors resulting in an increase of [^{18}F]FLT uptake can be manifold, including increased cellular proliferation (Ki67), DNA-salvage-pathway utilization (TK1), and DDR activity, as well as thymidine levels. These parameters might be modulated by tumor treatment, as demonstrated here for a FOLFOX combination therapy as well as a 5-FU monotherapy. Consequently, in this scenario, changes in [^{18}F]FLT reflect

alterations in these pathways, which are not directly related to tumor therapy response, as in general a reduced proliferation (and [^{18}F]FLT accumulation) is associated with tumor therapy response.

REFERENCES

1. Global Burden of Disease Cancer Collaboration, Fitzmaurice C, Dicker D, et al. The Global Burden of Cancer 2013. *JAMA Oncol*. 2015;1(4):505-527.
2. Longley DB, Harkin DP, Johnston PG. 5-fluorouracil: mechanisms of action and clinical strategies. *Nat Rev Cancer*. 2003;3(5):330-338.
3. Poon MA, O'Connell MJ, Wieand HS, et al. Biochemical modulation of fluorouracil with leucovorin: confirmatory evidence of improved therapeutic efficacy in advanced colorectal cancer. *J Clin Oncol*. 1991;9(11):1967-1972.
4. Raymond E, Faivre S, Woynarowski JM, Chaney SG. Oxaliplatin: mechanism of action and antineoplastic activity. *Semin Oncol*. 1998;25(2 Suppl 5):4-12.
5. André T, Boni C, Mounedji-Boudiaf L, et al. Oxaliplatin, fluorouracil, and leucovorin as adjuvant treatment for colon cancer. *N Engl J Med*. 2004;350(23):2343-2351.
6. Strauss LG. Fluorine-18 deoxyglucose and false-positive results: a major problem in the diagnostics of oncological patients. *Eur J Nucl Med*. 1996;23(10):1409-1415.
7. Schelhaas S, Heinzmann K, Bollineni VR, et al. Preclinical Applications of 3'-Deoxy-3'-[18F]Fluorothymidine in Oncology – A Systematic Review. *Theranostics*. 2017;7(1):40-50.
8. Bollineni VR, Kramer GM, Jansma EP, Liu Y, Oyen WJG. A systematic review on [18F]FLT-PET uptake as a measure of treatment response in cancer patients. *Eur J Cancer*. 2016;55:81-97.
9. Shields AF, Grierson JR, Dohmen BM, et al. Imaging proliferation in vivo with [F-18]FLT and positron emission tomography. *Nat Med*. 1998;4(11):1334-1336.
10. Toyohara J, Fujibayashi Y. Trends in nucleoside tracers for PET imaging of cell proliferation. *Nucl Med Biol*. 2003;30(7):681-685.
11. Zhang CC, Yan Z, Li W, et al. [(18)F]FLT-PET imaging does not always "light up" proliferating tumor cells. *Clin Cancer Res*. 2012;18(5):1303-1312.
12. Schelhaas S, Wachsmuth L, Viel T, et al. Variability of proliferation and diffusion in different lung

cancer models as measured by 3'-deoxy-3'-18F-fluorothymidine PET and diffusion-weighted MR imaging. *J Nucl Med*. 2014;55(6):983-988.

13. Schelhaas S, Heinzmann K, Honess DJ, et al. 3′-Deoxy-3′-[18F]Fluorothymidine Uptake Is Related to Thymidine Phosphorylase Expression in Various Experimental Tumor Models. *Mol Imaging Biol*. 2017:in press.
14. Bronckaers A, Gago F, Balzarini J, Liekens S. The dual role of thymidine phosphorylase in cancer development and chemotherapy. *Med Res Rev*. 2009;29(6):903-953.
15. Sinkus R, Van Beers BE, Vilgrain V, DeSouza N, Waterton JC. Apparent diffusion coefficient from magnetic resonance imaging as a biomarker in oncology drug development. *Eur J Cancer*. 2012;48(4):425-431.
16. Viel T, Schelhaas S, Wagner S, et al. Early assessment of the efficacy of temozolomide chemotherapy in experimental glioblastoma using [18F]FLT-PET imaging. *PLoS One*. 2013;8(7):e67911.
17. Heinzmann K, Honess DJ, Lewis DY, et al. The relationship between endogenous thymidine concentrations and [(18)F]FLT uptake in a range of preclinical tumour models. *EJNMMI Res*. 2016;6(1):63.
18. Podhorecka M, Skladanowski A, Bozko P. H2AX Phosphorylation: Its Role in DNA Damage Response and Cancer Therapy. *J Nucleic Acids*. 2010;2010:1-9.
19. Rubie C, Frick VO, Ghadjar P, et al. Effect of preoperative FOLFOX chemotherapy on CCL20/CCR6 expression in colorectal liver metastases. *World J Gastroenterol*. 2011;17(26):3109-3116.
20. Peters GJ, Backus HHJ, Freemantle S, et al. Induction of thymidylate synthase as a 5-fluorouracil resistance mechanism. *Biochim Biophys Acta - Mol Basis Dis*. 2002;1587(2-3):194-205.
21. Cassidy J, Tabernero J, Twelves C, et al. XELOX (capecitabine plus oxaliplatin): active first-line therapy for patients with metastatic colorectal cancer. *J Clin Oncol*. 2004;22(11):2084-2091.
22. Lee SJ, Kim SY, Chung JH, et al. Induction of thymidine kinase 1 after 5-fluorouracil as a mechanism for 3'-deoxy-3'-[18F]fluorothymidine flare. *Biochem Pharmacol*. 2010;80(10):1528-1536.
23. Li KM, Rivory LP, Hoskins J, Sharma R, Clarke SJ. Altered deoxyuridine and thymidine in plasma following capecitabine treatment in colorectal cancer patients. *Br J Clin Pharmacol*. 2007;63(1):67-

74.

24. Kenny LM, Contractor KB, Stebbing J, et al. Altered tissue 3'-deoxy-3'-[18F]fluorothymidine pharmacokinetics in human breast cancer following capecitabine treatment detected by positron emission tomography. *Clin Cancer Res*. 2009;15(21):6649-6657.

25. Hong YS, Kim HO, Kim K, et al. 3'-Deoxy-3'-18F-fluorothymidine PET for the early prediction of response to leucovorin, 5-fluorouracil, and oxaliplatin therapy in patients with metastatic colorectal cancer. *J Nucl Med*. 2013;54(8):1209-1216.

26. Yau K, Price P, Pillai RG, Aboagye E. Elevation of radiolabelled thymidine uptake in RIF-1 fibrosarcoma and HT29 colon adenocarcinoma cells after treatment with thymidylate synthase inhibitors. *Eur J Nucl Med Mol Imaging*. 2006;33(9):981-987.

27. Viertl D, Bischof Delaloye A, Lanz B, et al. Increase of [(18)F]FLT tumor uptake in vivo mediated by FdUrd: toward improving cell proliferation positron emission tomography. *Mol imaging Biol*. 2011;13(2):321-331.

28. Schelhaas S, Held A, Wachsmuth L, et al. Gemcitabine Mechanism of Action Confounds Early Assessment of Treatment Response by 3'-Deoxy-3'-[18F]Fluorothymidine in Preclinical Models of Lung Cancer. *Cancer Res*. 2016;76(24):7096-7105.

29. Chiu S-J, Lee Y-J, Hsu T-S, Chen W-S. Oxaliplatin-induced gamma-H2AX activation via both p53-dependent and -independent pathways but is not associated with cell cycle arrest in human colorectal cancer cells. *Chem Biol Interact*. 2009;182(2-3):173-182.

30. Saggar JK, Fung AS, Patel KJ, Tannock IF. Use of Molecular Biomarkers to Quantify the Spatial Distribution of Effects of Anticancer Drugs in Solid Tumors. *Mol Cancer Ther*. 2013;12(4):542-552.

31. Ikeda M, Kurose A, Takatori E, et al. DNA damage detected with gammaH2AX in endometrioid adenocarcinoma cell lines. *Int J Oncol*. 2010;36(5):1081-1088.

32. Löbrich M, Shibata A, Beucher A, et al. γH2AX foci analysis for monitoring DNA double-strand break repair: Strengths, limitations and optimization. *Cell Cycle*. 2010;9(4):662-669.

FIGURES

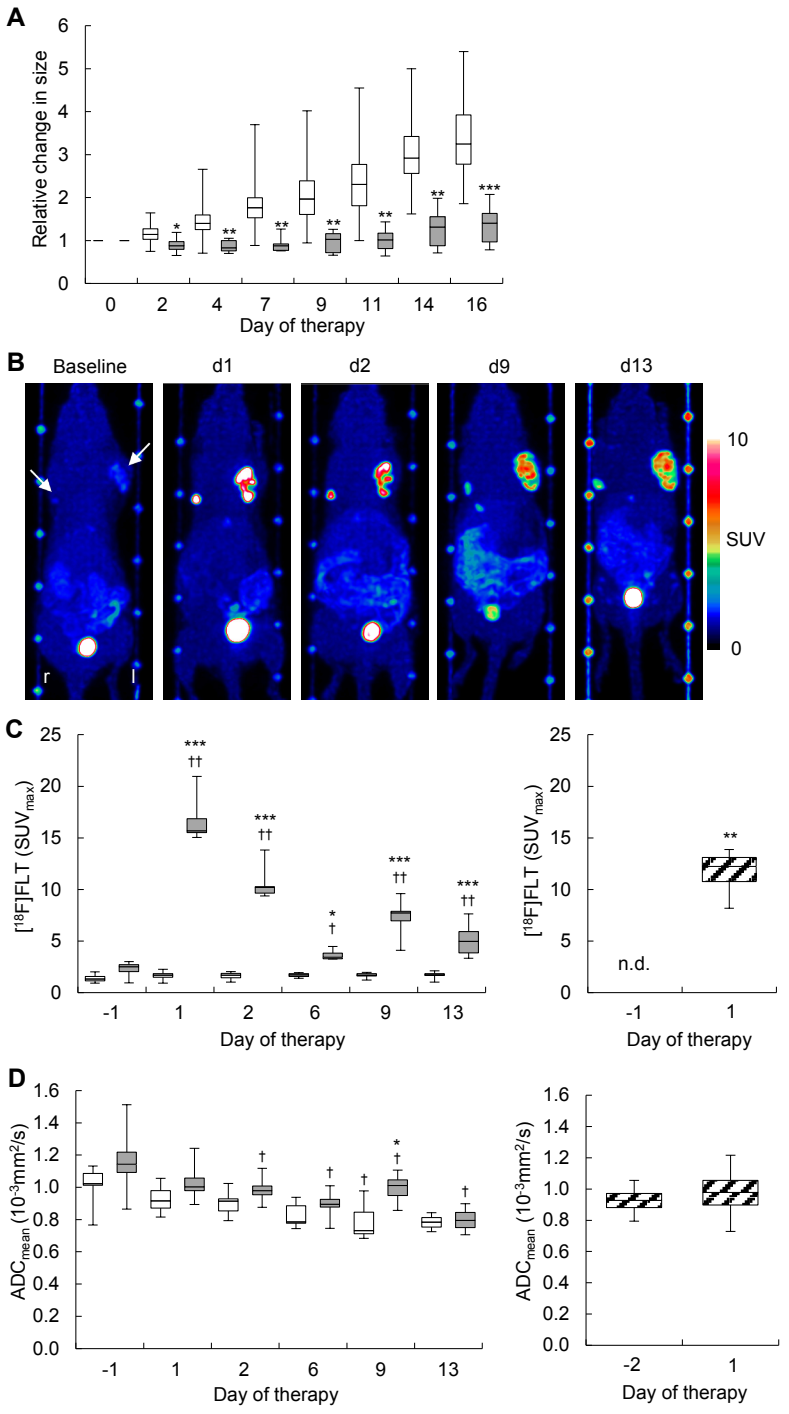

FIGURE 1. In Colo205 xenografts, FOLFOX therapy resulted in tumor growth arrest, increase in [^{18}F]FLT uptake and no increase in ADC_{mean}. (A) Caliper measurements revealed a growth inhibitory effect of FOLFOX, which was already significant on d2 of therapy. (B) Maximum-intensity-projections of a

representative FOLFOX treated mouse show that tumor [^{18}F]FLT uptake was remarkably enhanced after therapy. Imaging on d6 was not performed on the mouse presented here. The images also show the fiducial markers used for co-registration with MR images. Arrows point to the two tumors. (C) Quantification of tumor [^{18}F]FLT uptake revealed a remarkable increase of SUV_{max} relative to baseline after FOLFOX. (D) Significant reductions in ADC_{mean} relative to baseline could be observed during the growth of FOLFOX and control treated tumors. White: control, grey: FOLFOX, striped: 5-FU; *: $P < 0.05$, **: $P < 0.01$, ***: $P < 0.001$ relative to control; †: $P < 0.05$, ††: $P < 0.01$ relative to baseline.

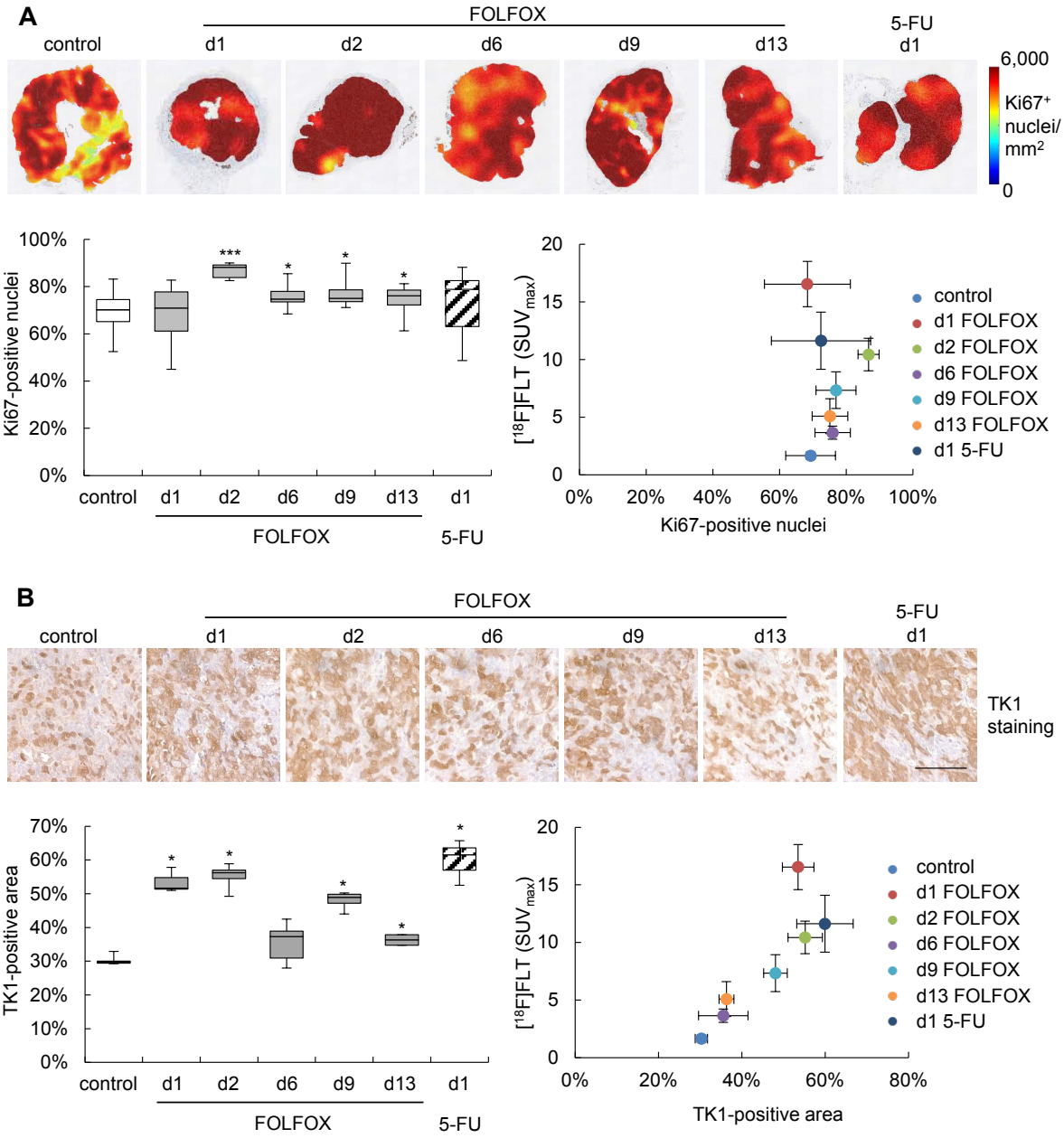

FIGURE 2. In Colo205 bearing mice, FOLFOX therapy resulted in an increase of histological proliferation markers. (A) Heatmaps depicting the density of Ki67-positive nuclei of representative tumors are shown in the upper panel. The percentage positive nuclei was quantified and related to [^{18}F]FLT uptake. (B) TK1 staining was quantified as positively stained area. Scale bar = 100 µm. White: control, grey: FOLFOX, striped: 5-FU; *: $P < 0.05$, ***: $P < 0.001$ relative to control.

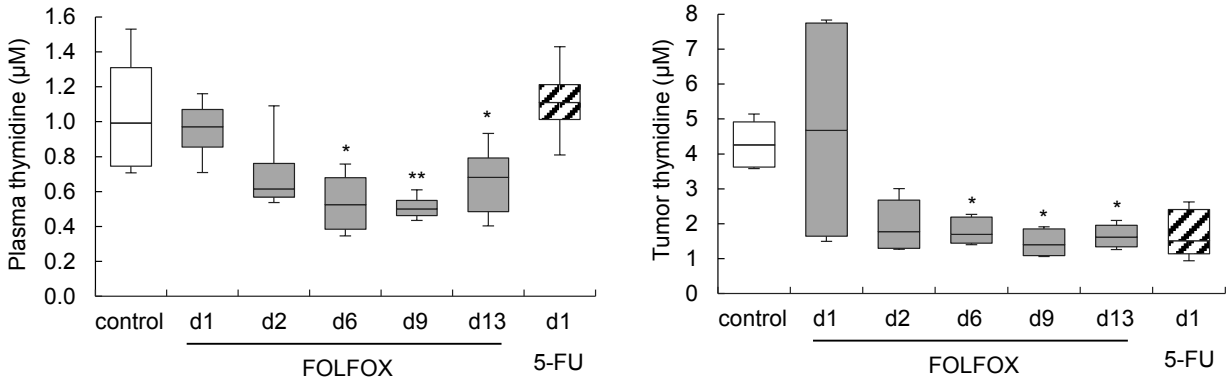

FIGURE 3. Thymidine levels were decreased in FOLFOX treated Colo205 tumors, as measured by liquid-chromatography-tandem mass spectrometry . White: control, grey: FOLFOX, striped: 5-FU; *: $P < 0.05$, **: $P < 0.01$ relative to control.

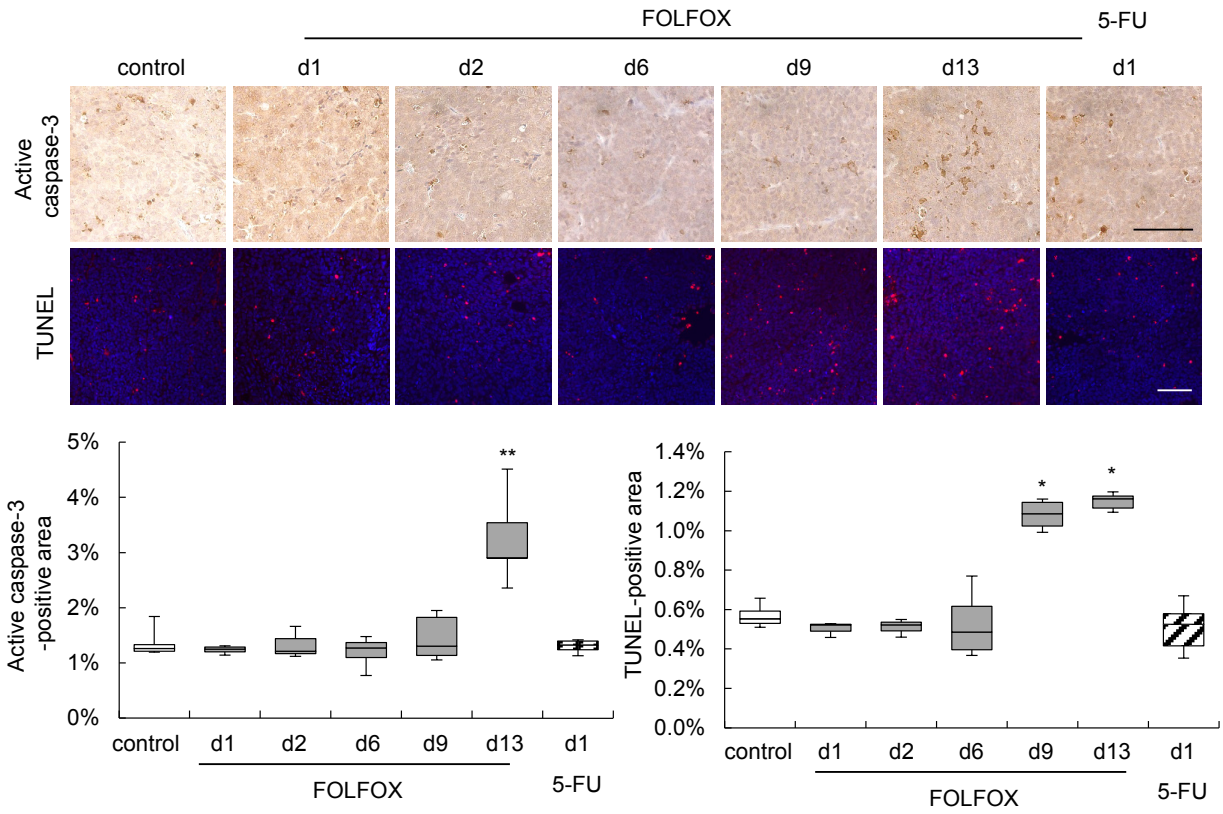

FIUGRE 4. Immunohistochemistry of activated caspase-3 and TUNEL assay of Colo205 tumors implied an increase in cell death after the second FOLFOX treatment. Scale bar = 100 μm. White: control, grey: FOLFOX, striped: 5-FU; *: $P < 0.05$, **: $P < 0.01$ relative to control.

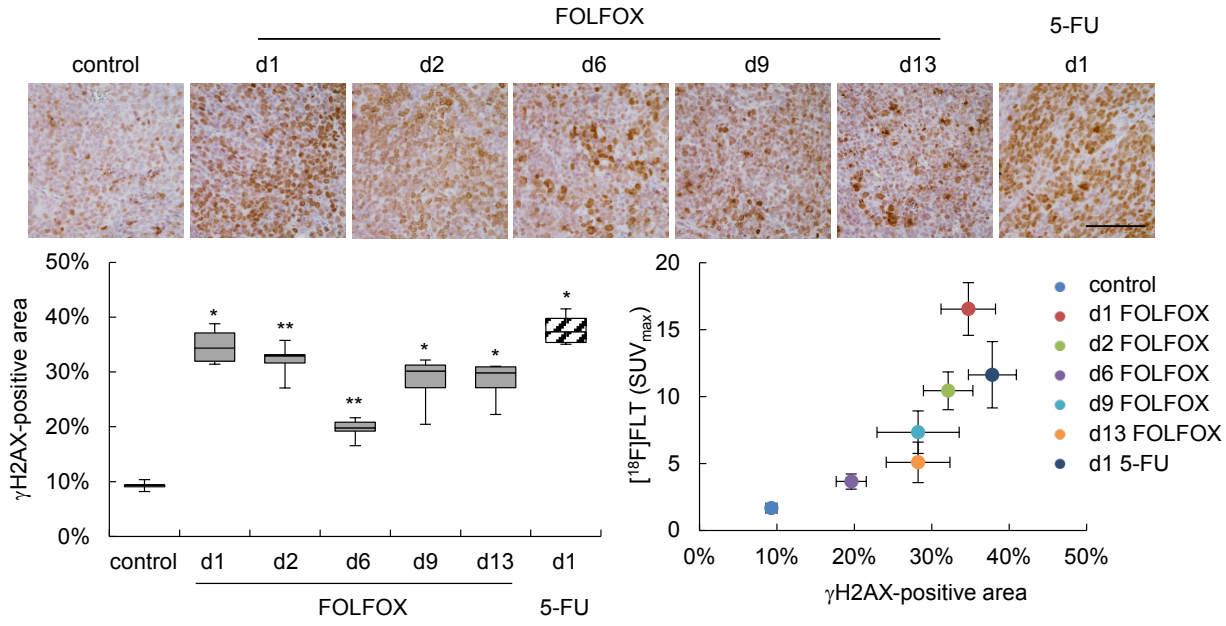

FIGURE 5. DDR is activated after FOLFOX therapy as determined by immunohistochemistry of γH2AX. The positively stained area was quantified and related to [^{18}F]FLT uptake. Scale bar = 100 µm. White: control, grey: FOLFOX, striped: 5-FU; *: $P < 0.05$, **: $P < 0.01$ relative to control.

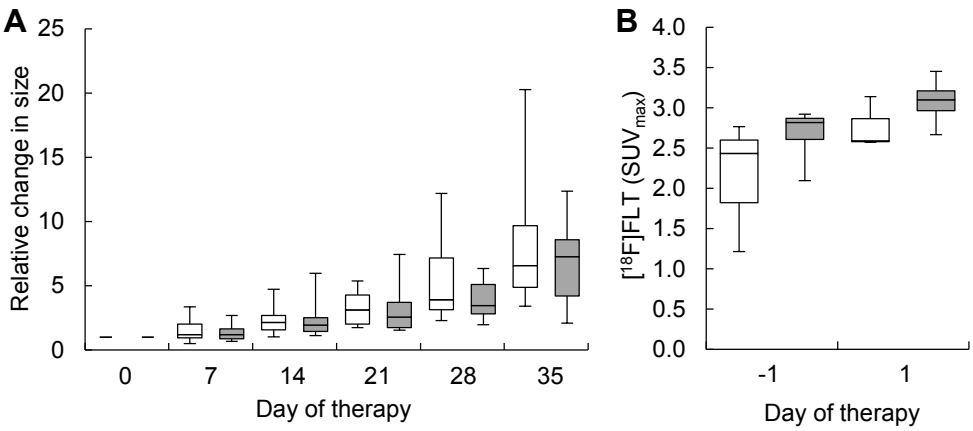

FIGURE 6. FOLFOX therapy in HCT116 xenografts affects neither tumor growth nor [^{18}F]FLT uptake. (A) Tumor volumes were determined by caliper measurements. Therapy was applied in weekly intervals. (B) [^{18}F]FLT accumulation was not significantly altered. White: control, grey: FOLFOX.

DISCLOSURE: The research leading to these results has received support from the Innovative Medicines Initiative Joint Undertaking (www.imi.europa.eu) under grant agreement number 115151.

ACKNOWLEDGEMENTS: We acknowledge Saeedeh Amirmohseni, Christine Bätza, Florian Breuer, Stefanie Bouma, Irmgard Hoppe, Sarah Köster, Christa Möllmann, Roman Priebe, and Dirk Reinhardt for excellent technical support.